

## RESEARCH ARTICLE

WILEY

# Soil-dependent $\beta$ and $\gamma$ shape parameters of the Haverkamp infiltration model for 3D infiltration flow

D. Yilmaz<sup>1</sup> | L. Lassabaterre<sup>2</sup> | D. Moret-Fernandez<sup>3</sup> | M. Rahmati<sup>4,5</sup> |  
R. Angulo-Jaramillo<sup>2</sup> | B. Latorre<sup>3</sup>

<sup>1</sup>Civil Engineering Department, Engineering Faculty, Munzur University, Tunceli, Turkey

<sup>2</sup>Univ Lyon, Université Claude Bernard Lyon 1, CNRS, ENTPE, UMR 5023 LEHNA, F-69518, Vaulx-en-Velin, France

<sup>3</sup>Departamento de Suelo y Agua, Estación Experimental de Aula Dei, Consejo Superior de Investigaciones Científicas (CSIC), Zaragoza, Spain

<sup>4</sup>Department of Soil Science and Engineering, Faculty of Agriculture, University of Maragheh, Maragheh, Iran

<sup>5</sup>Forschungszentrum Jülich GmbH, Institute of Bio- and Geosciences: Agrosphere (IBG-3), Jülich, Germany

## Correspondence

D. Yilmaz, Civil Engineering Department, Engineering Faculty, Munzur University, Tunceli, Turkey.

Email: [dyilmaz@munzur.edu.tr](mailto:dyilmaz@munzur.edu.tr)

## Abstract

Estimating of soil sorptivity ( $S$ ) and saturated hydraulic conductivity ( $K_s$ ) parameters by field infiltration tests are widespread due to the ease of the experimental protocol and data treatment. The analytical equation proposed by Haverkamp et al. (1994) allows the modelling of the cumulative infiltration process, from which the hydraulic parameters can be estimated. This model depends on both initial and final values of the soil hydraulic conductivity, initial soil sorptivity, the volumetric water content increase ( $\Delta\theta$ ) and two infiltration constants, the so-called  $\beta$  and  $\gamma$  parameters. However, to reduce the number of unknown variables when inverting experimental data, constant parameters such as  $\beta$  and  $\gamma$  are usually prefixed to 0.6 and 0.75, respectively. In this study, the values of these constants are investigated using numerical infiltration curves for different soil types and initial soil water contents for the van Genuchten-Mualem (vGM) soil hydraulic model. Our new approach considers the long-time expansions of the Haverkamp model, the exact soil properties such as  $S$ ,  $K_s$  and initial soil moisture to derive the value of the  $\beta$  and  $\gamma$  parameters for each specific case. We then generated numerically cumulative infiltration curves using Hydrus-3D software and fitted the long-time expansions to derive the value of the  $\beta$  and  $\gamma$  parameters. The results show that these parameters are influenced by the initial soil water content and the soil type. However, for initially dry soil conditions, some prefixed values can be proposed instead of the currently used values. If an accurate estimate of  $S$  and  $K_s$  is the case, then for coarse-textured soils such as sand and loamy sand, we propose the use of 0.9 for both constants. For the remaining soils, the value of 0.75 can be retained for  $\gamma$ . For  $\beta$  constant, 0.75 and 1.5 values can be considered for, intermediate permeable soils (sandy loam and loam) and low permeable soils (silty loam and silt), respectively. We clarify that the results are based on using the vGM model to describe the hydraulic functions of the soil and that the results may differ, and the assumptions may change for other models.

## KEYWORDS

Beerkan infiltration, Haverkamp model, Hydrus-3D synthetic soils, saturated hydraulic conductivity, soil sorptivity, steady-state

This is an open access article under the terms of the [Creative Commons Attribution-NonCommercial-NoDerivs](https://creativecommons.org/licenses/by-nc-nd/4.0/) License, which permits use and distribution in any medium, provided the original work is properly cited, the use is non-commercial and no modifications or adaptations are made.

© 2023 The Authors. *Hydrological Processes* published by John Wiley & Sons Ltd.

## 1 | INTRODUCTION

The quasi-exact implicit (QEI) three-dimensional (3D) analytical formulation for a disc infiltrometer infiltration with null or negative surface pressure (Haverkamp et al., 1994) is derived from the one-dimensional (1D) analytic approximation (AAP) proposed by Parlange et al. (1982), by including a new term representing the lateral flow (Smettem et al., 1994). This equation is expressed as a function of soil sorptivity,  $S$ , and hydraulic conductivity,  $K$ , volumetric water content increase,  $\Delta\theta$  and integration  $\beta$  and scale  $\gamma$  parameters.

The  $\beta$  parameter, which was initially introduced by Parlange et al. (1982) to derive the general form of the 1D QEI formulation, was next redefined by Haverkamp et al. (1990). According to Haverkamp et al. (1994),  $\beta$  is a function of the soil hydraulic conductivity, the soil diffusivity, and the initial and final volumetric water content. As for the constant  $\beta$ , several studies (Haverkamp et al., 1999; Ross et al., 1996) found it to be in the range of [0, 1], where 0 corresponds to soils with Green-Ampt (GA) behaviour, and one corresponds to very diffusive soils. This gave a physical interpretation to the integration parameter  $\beta$  depending on the soil type. However, the constant  $\beta$  value of 0.6 initially retained by Haverkamp et al. (1994), which was specific to their studied experimental sandy loam soil, became a default setting in almost all studies (Angulo-Jaramillo et al., 2016). This '0.6' value was calculated using soil textural information and the 1D analytical formulation (Fuentes et al., 1992). Some works have numerically investigated its optimal value with different results. When the QEI formulation (Lassabatere et al., 2009) or its expansions (Latorre et al., 2018; Moret-Fernández et al., 2020) were fitted to synthetic numerical curves generated for the Van Genuchten (1980) (vGM) soil hydraulic model,  $\beta$  increased from sand to diffusive soil type, exceeding the initially proposed range [0, 1].

The extension of the 1D AAP formulation to 3D formulation was performed by introducing the scaling factor  $\gamma$  (Smettem et al., 1994). The combination of the resolution for two-dimensional saturated water flow (known as the Laplace equation) and simplified assumptions such as GA wetting front during the infiltration process leads to a specific theoretical value of  $\sqrt{0.3}$  for  $\gamma$  (Smettem et al., 1994). Since this theoretical value was specific to a GA wetting front, the  $\gamma$  value was corrected to 0.75 to fit the 3D formulation to their experimental soil data (Smettem et al., 1994). Then, the 0.75 value for  $\gamma$  became a common value for many studies (Di Prima et al., 2020; Yilmaz, 2021; Yilmaz et al., 2022). However, according to Haverkamp et al. (1994), this parameter should be constrained within the [0.6, 0.8] range.

The proper values of  $\beta$  and  $\gamma$  parameters are the subject of discussion because both are known to depend on soil type and initial water content (Angulo-Jaramillo et al., 2016; Lassabatere et al., 2009) rather than being considered unique values. As described above, several studies have evaluated the values of  $\beta$  and  $\gamma$  separately, however, to date, no study has focused on the simultaneous estimation of  $\beta$  and  $\gamma$ . In general, the  $\beta$  parameter is prefixed according to measurements performed in a 1D vertical column in the laboratory or directly calculated by the analytical formula of Fuentes et al. (1992). Then  $\gamma$  is

adjusted or optimized with the  $S$  and  $K_s$  estimations. Therefore, this paper is novel because it aims to investigate simultaneously the optimal values of  $\beta$  and  $\gamma$  parameters. This approach differs from the others since it does not constrain the optimized couplet to 1D flow estimation. For this purpose, numerical cumulative infiltration curves corresponding to six different synthetic soils from the database of and with contrasting hydraulic behaviours are considered. Hydrus-3D software was used to model cumulative infiltration corresponding to a zero water pressure head at the surface, considering the vGM model for describing the soil hydraulic functions and several initial water contents. The long-time expansion of QEI formulation was used to retrieve the couplet of unknown  $\beta$  and  $\gamma$  for each synthetic soil. Then, the variation of both parameters is discussed in the function of the synthetic soils and initial soil water conditions.

## 2 | MATERIALS AND METHODS

### 2.1 | Soil hydraulics functions

The van Genuchten model uses the following mathematical function to describe the water retention (Equation 1a) and the hydraulic conductivity (Equation 1b) curves:

$$S_e = \frac{\theta - \theta_r}{\theta_s - \theta_r} = [1 + |\alpha h|^n]^{-m}, \quad (1a)$$

$$K(\theta) = K_s \left( \frac{\theta - \theta_r}{\theta_s - \theta_r} \right)^l \left[ 1 - \left( 1 - \left( \frac{\theta - \theta_r}{\theta_s - \theta_r} \right)^{\frac{1}{m}} \right)^2 \right], \quad (1b)$$

$$m = 1 - \frac{k_m}{n}, \quad (1c)$$

where  $S_e$  is the degree of soil water saturation,  $\theta$  ( $L^3 L^{-3}$ ) is the volumetric soil water content,  $h$  (L) is the water pressure head,  $K$  ( $L T^{-1}$ ) is the soil hydraulic conductivity,  $n$  and  $m$  are shape parameters,  $k_m$  is a user index (Haverkamp et al., 2016),  $l$  is a tortuosity parameter and  $\alpha$  ( $L^{-1}$ ) representing the inflection point of the water retention curve,  $\theta_s$  and  $\theta_r$  ( $L^3 L^{-3}$ ) are saturated and residual soil volumetric water contents, and  $K_s$  ( $L T^{-1}$ ) is the field-saturated soil hydraulic conductivity. The Mualem condition (1976) set the  $k_m$  parameter to 1 and  $l$  to 0.5.

### 2.2 | Synthetic data from Hydrus-3D software

Cumulative Beerkan infiltrations were simulated using HYDRUS-2D/3D software (Šimůnek et al., 2008), which solves Richards' equation governing the flow by applying the finite element method. The numerical domain was configured as a cylinder of 40 cm radius and 40 cm height, representing a volume of 200 dm<sup>3</sup>, large enough to contain the wetting front below the ring infiltration device during the whole infiltration process until the attainment of steady-state. Finite

**TABLE 1** vGM related hydraulic parameters for the six studied synthetic soils (Di Prima et al., 2021).

Type of soil	$\theta_r$	$\theta_s$	$n$	$\alpha$ (cm <sup>-1</sup> )	$K_s$ (cm.min <sup>-1</sup> )	$t_f$ (min)
Sand	0.045	0.430	2.68	0.145	0.495	30
Loamy sand	0.057	0.410	2.28	0.124	0.2432	60
Sandy loam	0.065	0.410	1.89	0.075	0.07368	120
Loam	0.078	0.430	1.56	0.036	0.01733	240
Silty loam	0.067	0.450	1.41	0.02	0.00750	480
Silt	0.034	0.460	1.37	0.016	0.00417	720

elements of 2 mm were used to discretize the numerical domain (Lassabatere et al., 2009). The upper boundary condition was set to saturated water content for the ring section, while the lower boundary limit was set to free drainage condition, and zero flux boundary conditions were applied elsewhere. The ring radius  $r_d$  was set to 5 cm. The vGM model and related hydraulic properties of six synthetic soils, ranging from sand to silt textures, were used (Table 1). The initial water content was considered homogeneous and set to a degree of saturation  $S_e$  of 0, 0.1, 0.2, 0.3 and 0.4. Because of numerical problems for sand and loamy sand, the initial degree of saturation 0 was replaced by 0.05.

### 2.3 | Detection of steady-state

Di Prima et al. (2021) introduced the approach to detect the attainment of steady-state. First, the program considers the last four points of the infiltration curve and then performs a linear regression to calculate the slope. The latter is considered the reference slope. Then the program increments by one the number of points to be considered for the linear regression. At each increment, a threshold  $E$  is calculated as follows:

$$E = \frac{\text{slope\_last}_i - \text{slope\_reference}}{\text{slope\_reference}} < 0.005, \quad (2)$$

where  $\text{slope\_last}_i$  and  $\text{slope\_reference}$  values are the measured slope, including the last  $i$ th and fourth points, respectively. The points respecting the threshold are considered for the long-time regime. When the threshold value becomes higher than 0.005 for an incremented  $i$  number of points, the algorithm stops and considers the steady-state flow process starting at the  $i + 1$  points of the cumulated infiltration curve.

### 2.4 | QEI infiltration formulation and its long-time approximation

For a given initial volumetric water content,  $\theta_i$ , the QEI formulation models the cumulative infiltration at the surface of a single ring of radius  $r_d$  (Beerkan type experiment) as below (Haverkamp et al., 1994):

$$\frac{2\Delta K^2}{S^2}t = \frac{1}{1-\beta} \left( \frac{2\Delta K}{S^2} \left( I_{3D} - \frac{\gamma S^2}{r_d(\theta_s - \theta_i)}t - K_i t \right) - \ln \left( \frac{e^{\frac{2\beta\Delta K}{S^2} \left( I_{3D} - \frac{\gamma S^2}{r_d(\theta_s - \theta_i)}t - K_i t \right)} + \beta - 1 \right) \right), \quad (3)$$

Where  $t$  (T) is the time,  $I_{3D}$  (L) is the cumulative 3D infiltration,  $\gamma$  is the scaling constant representative of the lateral flow,  $\beta$  is the integration parameter,  $S$  (L T<sup>-0.5</sup>) is the initial soil sorptivity,  $K_i$  is the initial soil hydraulic conductivity, and  $\Delta K$  is the difference between the saturated and the initial soil hydraulic conductivity. For long times, the 3D cumulative infiltration,  $I_{+\infty}$  (L), can be approximated by the following explicit steady-state expansion (Haverkamp et al., 1994):

$$I_{+\infty}(t) = (AS^2 + \Delta K) \cdot t + C \frac{S^2}{\Delta K}. \quad (4a)$$

For the specific case of the vGM model,  $A$  (L<sup>-1</sup>) and  $C$  constants are defined as:

$$A = \frac{\gamma}{r_d(\theta_s - \theta_i)}, \quad (4b)$$

$$C = \frac{1}{2(1-\beta)} \ln \left( \frac{1}{\beta} \right). \quad (4c)$$

### 2.5 | Reference S calculation, estimation from the steady-state shape, and S error objective function

The reference sorptivity  $S_{ref}$  is calculated using the Parlange (1975) flux concentration model as follows:

$$S_{ref}^2(\theta_0, \theta_i) = \int_{\theta_i}^{\theta_0} (\theta_0 + \theta - 2\theta_i) D(\theta) d\theta, \quad (5a)$$

where  $D$  stands for the soil diffusivity function. The  $S_{ref}$  is calculated for each synthetic soil (Table 1) and initial soil water content using the computation algorithm proposed by Lassabatere et al. (2023).

Alternatively,  $S$  can be related to the slope and intercept coefficient of Equation (4a) as follows (Bagarello et al., 2014):

$$S = \sqrt{\frac{S_{std}}{A + \frac{C}{i_{std}}}} \quad (5b)$$

where  $S_{std}$  and  $i_{std}$  stand for the slope and the intercept of the linear regression of the steady-state part of the cumulated infiltration curve. The Equation (5b) defines sorptivity as a function of the  $\beta$  and  $\gamma$  parameters.  $S$  defined by Equation (5b) must equal  $S_{ref}$  as defined by Equation (5a). We then assess the objective function to calculate the deviation from the reference value as follow:

$$S_{error} = S_{ref} - \sqrt{\frac{S_{std}}{A + \frac{C}{i_{std}}}} \quad (5c)$$

Accurate values of the  $\beta$  and  $\gamma$  parameters must ensure values of the optimization function close to zero.

## 2.6 | $K_s$ estimation from the steady-state and $K_s$ error objective function

$K_s$  is estimated from Equation (4a) using the intercept information (Yilmaz et al., 2010) as follows:

$$K_s = \frac{S_{std}}{\left(i_{std} \cdot \frac{A}{C} + 1\right) \left(1 - \left(\frac{\theta_i - \theta_r}{\theta_s - \theta_r}\right)^{0.5} \left[1 - \left(1 - \left(\frac{\theta_i - \theta_r}{\theta_s - \theta_r}\right)^{\frac{1}{m}}\right)^{m-2}\right]\right)} \quad (6a)$$

The objective function to calculate the deviation from the reference value is defined as follows:

$$K_{serror} = K_{sref} - \frac{S_{std}}{\left(i_{std} \cdot \frac{A}{C} + 1\right) \left(1 - \left(\frac{\theta_i - \theta_r}{\theta_s - \theta_r}\right)^{0.5} \left[1 - \left(1 - \left(\frac{\theta_i - \theta_r}{\theta_s - \theta_r}\right)^{\frac{1}{m}}\right)^{m-2}\right]\right)} \quad (6b)$$

Again, accurate values of the  $\beta$  and  $\gamma$  parameters must ensure values of the optimization function close to zero. We have then defined two objective functions that allow retrieving the best values of the  $\beta$  and  $\gamma$  parameters.

## 2.7 | Contours of the minimum of $K_s$ and $S$ error objective function

$K_s$  and  $S$  are estimated for  $(\beta, \gamma)$  couplets ranging each term from 0.1 to 3 with an increment step of 0.005. Thus, the objective function is calculated for each couplet to find the minimum. Crossing the objective functions thus takes up the values of  $(\beta, \gamma)$  couplet that best fits with the values of references  $K_s$  and  $S$ . Since the objective functions (5a and 6b) are derived from the shape coefficient of the steady-state, the calculation of the values of  $(\beta, \gamma)$  are done from the shape coefficient as described after.

## 2.8 | Estimation of $(\beta, \gamma)$ couplet from shape coefficient

The  $\gamma$  value is calculated by considering the relation (4a) with the reference values  $K_s$  and  $S$ , and the slope of the linear regression of the steady-state points as follows:

$$\gamma = \frac{r_d(\theta_s - \theta_i)(S_{std} - K_{sref})}{S_{ref}^2} \quad (7a)$$

In order to calculate the  $\beta$  value, the intercept of the regression line of the steady-state is used to define a new objective function  $f$ , as follows:

$$f(\beta) = i_{std} - \frac{1}{2(1-\beta) \left(1 - \left(\frac{\theta_i - \theta_r}{\theta_s - \theta_r}\right)^{0.5} \left[1 - \left(1 - \left(\frac{\theta_i - \theta_r}{\theta_s - \theta_r}\right)^{\frac{1}{m}}\right)^{m-2}\right]\right)} \ln\left(\frac{1}{\beta}\right) \frac{S_{ref}^2}{K_{sref}} \quad (7b)$$

Then Scilab 'fsolve' function (Campbell et al., 2010), which finds the zero for a mathematical function, is used to retrieve the equivalent  $\beta$ . The values of the  $(\beta, \gamma)$  couplet computed with Equations (7a) and (7b) correspond to the optimum values of the objective functions defined by Equation (5c).

## 2.9 | Relative error estimation of $S$ and $K_s$ using by-default $(\beta, \gamma)$ couplet

To highlight the bias in the estimation of  $S$  and  $K_s$  with respect to their reference value, when the by-default  $(\beta = 0.6, \gamma = 0.75)$  couplet is used, the relative error (%) is calculated as follows:

$$S_{relative\ error} = \frac{S_{estimated} - S_{ref}}{S_{ref}} \times 100 \quad (8a)$$

$$K_{srelative\ error} = \frac{K_{sestimated} - K_{sref}}{K_{sref}} \times 100 \quad (8b)$$

## 3 | RESULTS

### 3.1 | Beerkan cumulative infiltrations and steady-state asymptotes

Simulations for the six synthetic soils and the different scenarios of initial water content are shown in Figure 1. The steady-state attainment time,  $t_{std}$ , asymptote slope,  $s_{std}$  and intercept,  $i_{std}$ , are summarized in Table 2.

### 3.2 | Contour of objectives functions

The contours of the objective error functions for  $S$  (Equation 5c) and  $K_s$  (Equation 6b) and the intersection of both contour error lines of

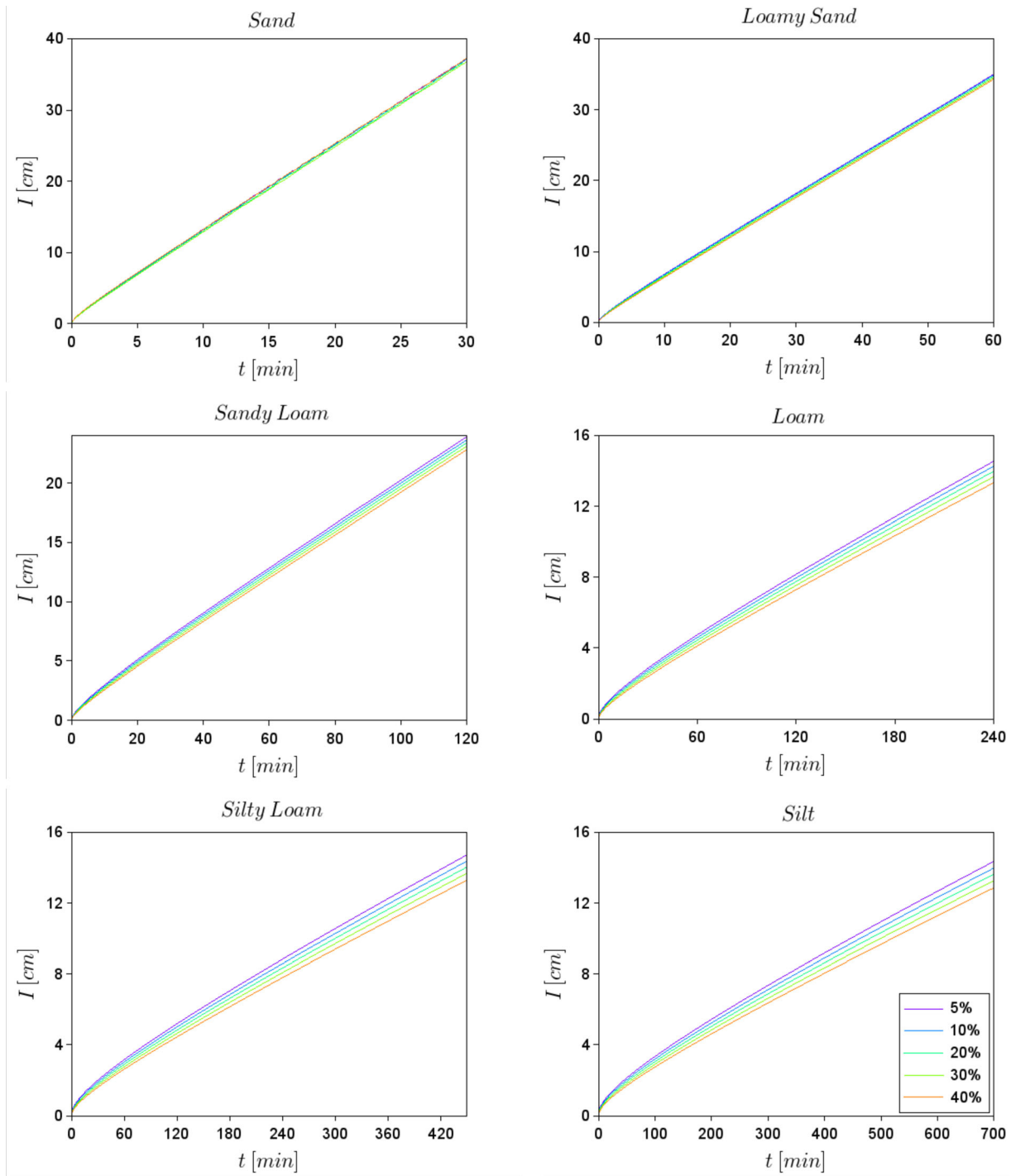


**FIGURE 1** Numerical H3D Beerkan Cumulated infiltration for the six synthetic soils and scenarios of initial soil water volumetric content of 5%, 10%, 20%, 30% and 40% of the effective soil water storage capacity ( $\theta_s - \theta_i$ ).

0.005 for initial saturation degree  $S_e = 0.1$  are illustrated in Figure 2. The crossing pattern (Right column, Figure 2) shows the  $(\beta, \gamma)$  couplet that fits well with both expected  $S$  and  $K_s$  values. Their exact values were calculated from steady-state shape coefficients and summarized in Table 2 (Cf. the last two columns).

### 3.3 | Relative error of $S$ and $K_s$ estimates using by-default values of $(\beta, \gamma)$ couplet

Using the by-default value of 0.6 and 0.75 for  $(\beta, \gamma)$  couplet resulted in relative errors for  $S$  estimate below 2%, in absolute value, for sand,

**TABLE 2** Summary of asymptote slope and intercept, relative error on  $S$  and  $K_s$  using by-default  $(\beta, \gamma)$  estimated optimum values of  $(\beta, \gamma)$ .

	$S_{ei}$ (–)	$t_{std}$ (min)	$s_{std}$ (mm.min <sup>-1</sup> )	$i_{std}$ (mm)	$S$ Equation (5a) (mm.min <sup>-0.5</sup> )	$S_{error}$ Equation (8a) (%)	$K_{serror}$ Equation (8b) (%)	$\beta$ Equation (7b)	$\gamma$ Equation (7a)
Sand	0.05	11.3	1.198	1.319	1.148	0.8	31.0	1.020	0.975
	0.1	11.7	1.197	1.251	1.116	0.9	30.9	1.012	0.976
	0.2	9.4	1.197	1.090	1.049	0.7	32.2	1.042	0.982
	0.3	7.5	1.196	0.934	0.977	0.5	33.9	1.076	0.990
Loamy sand	0.05	23.5	0.561	1.378	0.773	1.5	17.3	0.792	0.890
	0.1	23.2	0.560	1.302	0.752	1.5	17.4	0.793	0.892
	0.2	19.8	0.560	1.141	0.706	1.4	18.1	0.806	0.896
	0.3	17.9	0.559	0.989	0.658	1.6	18.7	0.809	0.902
	0.4	15.8	0.558	0.835	0.605	1.8	20.2	0.821	0.913
Sandy loam	0	68.3	0.184	1.835	0.491	-1.3	11.1	0.794	0.789
	0.1	64.5	0.183	1.667	0.465	-1.1	10.0	0.770	0.787
	0.2	64.9	0.182	1.515	0.437	-0.5	8.1	0.725	0.786
	0.3	64.0	0.181	1.369	0.407	0.4	5.6	0.665	0.785
	0.4	55.0	0.180	1.185	0.374	1.0	4.7	0.635	0.789
Loam	0	159.0	0.053	1.944	0.285	-7.2	32.1	1.429	0.766
	0.1	161.0	0.052	1.814	0.269	-6.9	27.8	1.322	0.756
	0.2	167.0	0.051	1.688	0.253	-6.3	22.8	1.196	0.746
	0.3	159.0	0.051	1.534	0.236	-5.8	18.6	1.093	0.738
	0.4	155.0	0.050	1.362	0.217	-5.2	14.6	0.996	0.731
Silty loam	0	338.0	0.028	2.337	0.222	-8.5	50.8	1.923	0.775
	0.1	327.0	0.027	2.182	0.211	-8.4	45.3	1.785	0.761
	0.2	328.0	0.027	2.019	0.198	-8.0	39.8	1.642	0.751
	0.3	346.0	0.026	1.867	0.185	-7.5	32.9	1.462	0.738
	0.4	266.0	0.026	1.591	0.170	-7.5	32.1	1.448	0.737
Silt	0	560.0	0.017	2.511	0.184	-9.4	70.4	2.465	0.800
	0.1	556.0	0.017	2.332	0.175	-9.3	64.6	2.317	0.786
	0.2	525.0	0.016	2.127	0.164	-9.2	60.1	2.193	0.777
	0.3	523.0	0.016	1.944	0.153	-8.8	53.4	2.004	0.765
	0.4	266.0	0.026	1.591	0.170	-7.5	32.1	1.813	0.737

loamy sand, and sandy loam (Table 2). For the others, the error was constrained below 10% in absolute value. For  $K_s$  estimates, the relative errors were higher than for  $S$  estimates. The minimum error range was observed for sandy loam in the range of (4.7–11.1) %, and the maximum error was for silt in the range of (32.1–70.4) % in function to the initial degree of saturation.

### 3.4 | Identification of $(\beta, \gamma)$ couplet from steady-state measurements

For initial conditions of  $S_e = 0.1$ , parameter  $\beta$  depends on the soil texture and decreases from 1.01 to 0.77, respectively, for sand and sandy loam and then increases to 2.32 for silt (Table 2). This parameter also increases from dry to wetter initial conditions for loamy sand, whereas it decreases for the other synthetic soils.

The value of the  $\gamma$  parameter for an initial degree of saturation of 0.1 decreases from 0.98 to 0.76 for sand and loam, respectively, and then it slightly increases to 0.79 for silt. For sand and loamy sand,  $\gamma$  optimized values slightly increase from dry to wetter initial conditions and decrease for the remaining soils.

## 4 | DISCUSSION

### 4.1 | Effect of the by-default couplet value on the estimates of $K_s$ and $S$

The objective error function for  $K_s$  (Figure 2) obtained from the steady-state approach (Equation 4a) shows an increasing elongated valley, which indicates that infinite values of the couplet  $(\beta, \gamma)$  can be chosen for the actual estimate of  $K_s$ . A similar behaviour, with a

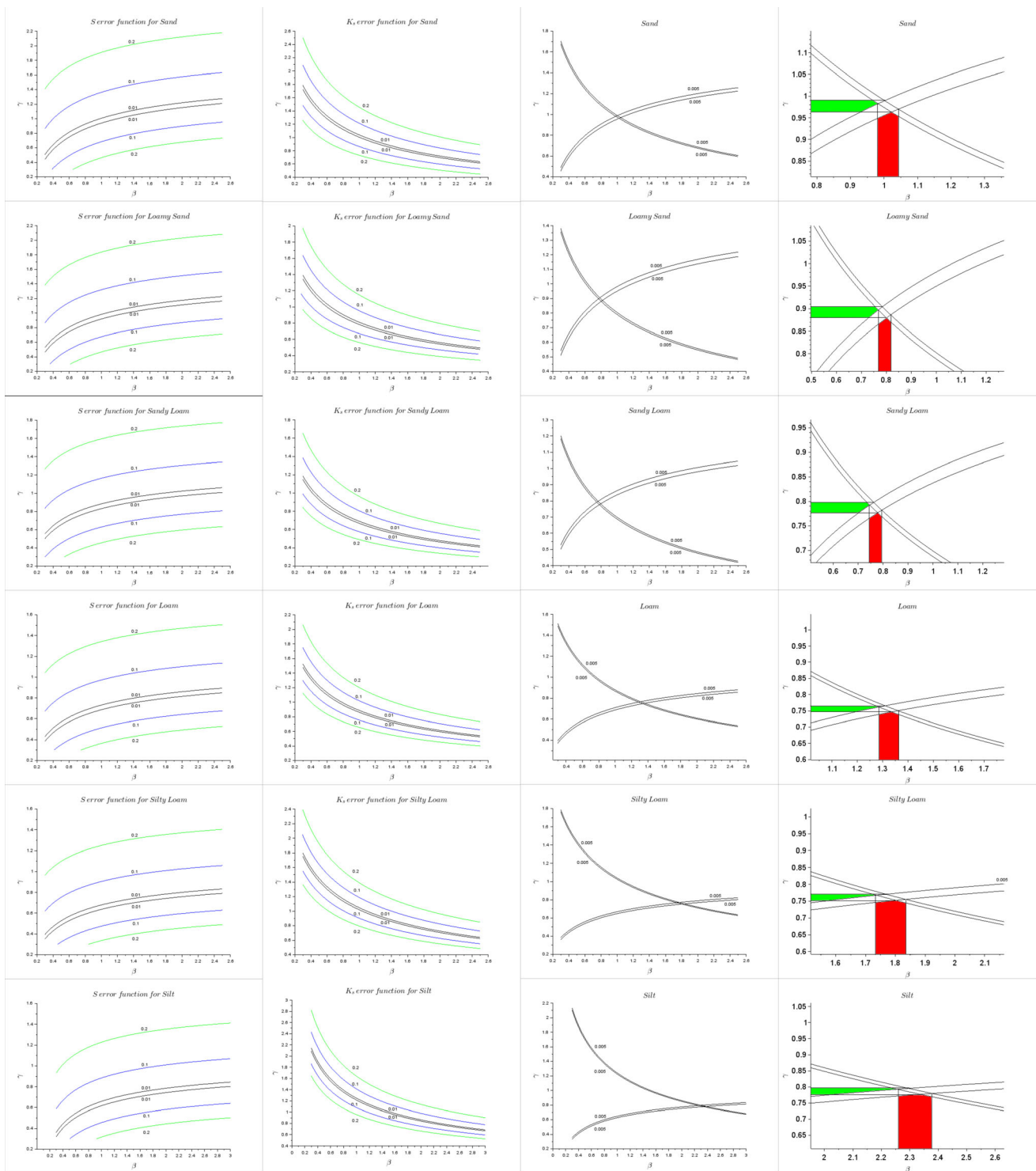


**FIGURE 2**  $S$  and  $K_s$  error functions contours for 0.1 initial degree of saturation, (the green, blue and black lines represent respectively error value of 0.2, 0.1 and 0.01) and error functions intersection for  $S$  and  $K_s$  and for 0.005 error value.

decreasing elongated valley, was observed in the estimates of  $S$ . Simultaneous estimate of both parameters conducts to a restricted choice of the couplet  $(\beta, \gamma)$  represented by the intersection of both valleys with minimum error. Identifying the intersection of the two zones correctly identifies the optimum values of the couplet  $(\beta, \gamma)$  and are directly calculated from Equations (7a) and (7b). Therefore, it is

interesting to test the by-default  $(\beta, \gamma)$  couplet value to see the potential errors in the estimation of  $S$  and  $K_s$  (Table 2). In such case and considering the field variability of intrinsic soil parameters such as porosity, the relative errors observed for  $S$  are negligible ( $<10\%$ ). For the estimation of  $K_s$ , the observed relative error is higher than  $S$ , but indicates that the estimates remain in the same order of magnitude as

the reference value (<60%). The case of synthetic sandy loam, with the by-default couplet  $(\beta, \gamma)$ , led to the smallest errors. That seems logical since the original default values were calculated for cumulative infiltration curves experimentally measured for sandy loam soils in the laboratory (Smettem et al., 1994) and on the field (Haverkamp et al., 1994). Globally, for a more rigorous estimation of the  $K_s$  parameter, the couplet  $(\beta, \gamma)$  must be corrected according to the soil type and initial soil moisture content.

## 4.2 | Comparison to values of couplet $(\beta, \gamma)$ reported in the literature

In the literature, almost all studies that employ the QEI formulation (Haverkamp et al., 1994) and its corresponding expansions systematically used the by-default  $(\beta, \gamma)$  values. Note that BEST methods (Di Prima et al., 2021; Yilmaz et al., 2019) and the simplified Beerkan approach (Bagarello et al., 2017; Di Prima et al., 2020; Yilmaz, 2021) used a different model for the modelling of hydraulic functions, that is, the van Genuchten (1980) model for the water retention curve and the Brooks and Corey (1964) model for the unsaturated hydraulic conductivity (Lassabatere et al., 2021). Therefore, the conclusion of this study may not apply to these methods since we investigated values of  $(\beta, \gamma)$  for the specific case of the vGM model. However, we may expect similar trends. Further investigations will deal with the dependency of our findings on the mathematical formulations considered for the description of the water retention and hydraulic conductivity functions.

Few studies have evaluated the effect of  $\beta$  and  $\gamma$  parameters on the estimates of  $K_s$  and  $S$  (Table 3), focusing mainly on initial very dry conditions. Our study differs from these in that we analysed the

cumulative infiltration at long times, we estimate simultaneously both parameters  $\beta$  and  $\gamma$  rather than fixing  $\beta$  from 1D and adjusting  $\gamma$  value. In complement, we also investigate the effect of initial soil moisture from dry to wet conditions on both parameters. For instance, Latorre et al. (2018) observed that  $\beta$  could be accurately estimated with QEI formulation from a single infiltration curve only when very long times were considered. Once  $\beta$  is estimated then they extrapolated the 1D results to 3D flow. Similar approach was done by Lassabatere et al., 2009. Working with QEI expansions, Moret-Fernández et al. (2020) and Rahmati et al. (2020) prefixed  $\beta$  according to textural parameters and 1D analytical formulation of Fuentes et al. (1992). They observed that  $\beta$  had a meagre impact on the  $K_s$  and  $S$  estimates. However, using the long-time formulation, we observed that the  $\beta$  parameter has a direct influence on the coefficient  $C$  (Equation 4c), which directly influences the estimation of  $K_s$  and  $S$ . This results in significant differences between the  $\beta$  values in the literature obtained from 1D flow conditions and those found in this work for 3D flow conditions.

For sand synthetic soil, the  $\beta$  value observed for initially relatively dry soils was close to 1.02. This value differs from the study of Lassabatere et al. (2009), Rahmati et al. (2020) and Moret-Fernández and Latorre (2017), who observed  $\beta$  value between 0.33 and 0.6. Note that although Moret-Fernández et al. (2020) considered  $\beta$  value of 0.6 for sandy soils from inversion of 1D infiltration experiments, for 3D infiltration, the  $\beta$  value observed in their optimization procedure was close to 1. This clearly shows differences between the 1D and 3D  $\beta$  estimates and calls into question the extrapolation of  $\beta$  from 1D flow to estimate soil parameters from the 3D flow.

For the  $\gamma$  parameter, our observed values are close to those proposed by Lassabatere et al. (2009). Moreover, Moret-Fernández et al.

	Synthetic soil	$\beta$	$\gamma$
Lassabatere et al. (2009)—From QEI 3D infiltration	Sand	0.33	1.030
	Loam	1.25	0.756
	Silt	1.56	0.748
Moret-Fernández and Latorre (2017)—From Upward 1D infiltration	Sand	0.63	
	Loam	1.25	
	Silt	1.56	
Latorre et al. (2018)—From AAP 1D infiltration	Loamy sand	0.78	
	Loam	1.27	
	Silt	1.50	
Moret-Fernández et al. (2020)—From QEI 3D infiltration	Sand	0.63	1.030
	Loam	1.25	0.756
	Silt	1.56	0.748
Rahmati et al. (2020)—From 5T expansion of AAP 1D infiltration	Sand	0.60	
	Loamy sand	0.80	
	Sandy loam	0.99	
	Loam	1.27	
	Silty loam	1.44	
	Silt	1.50	

**TABLE 3** Literature summary of optimized  $\beta$  or/and  $\gamma$  parameters on numerical curves produced with vGM model from Hydrus software and QEI formulation and its expansions.



(2020) reused the  $\gamma$  value for loam soil and observed similar optimized values of  $\beta$  in comparison to our steady-state approach. Haverkamp et al. (1994) bounded  $\gamma$  parameter between 0.6 and 0.8 for 'normal working conditions'. This statement is vague since 'normal working condition' is not explicit. It seems that for very permeable soil, such as sand and loamy sand, this range can be expanded and be closer to 1.

### 4.3 | Effect of the initial soil water content

#### 4.3.1 | On the estimate of $S$ and $K_s$ using the by-default couplet ( $\beta, \gamma$ )

Regarding the effect of the initial water content with the by-default couplet ( $\beta, \gamma$ ), a similar error was obtained in the estimation of  $S$ , regardless of the initial soil water content (Table 2). Therefore, no effect of the initial water content was observed for this parameter. Contrary to the estimation of  $K_s$ , the increase of the initial water content resulted in an increase or a decrease in the error according to the soil type (Table 2). For instance, for sand and loamy soils, the error of  $K_s$  remains almost stable with the increase of the initial soil degree saturation. This trend contrasts with the remaining soils, where a decrease of the  $K_s$  error with the increase of the initial soil degree saturation was observed. Therefore, the studied synthetic soils could be classified into two groups: sand and loamy sand soils on the one hand, and sandy loam, loam, silty loam and silt soil on the other hand, with regard to the impact of the by-default value on the estimations of  $S$  and  $K_s$ . The evolution of the optimum values of the couplet ( $\beta, \gamma$ ) is then discussed afterwards.

#### 4.3.2 | On the optimized value of ( $\beta, \gamma$ )

For the first group,  $\beta$  and  $\gamma$  values increase with increasing initial water content. It should be noted that the increase of  $\gamma$  is contained in a small range (Table 2) compared to  $\beta$  and can be considered almost constant. For the second group, we have an opposite effect where  $\beta$  and  $\gamma$  values decrease with the increase of the initial water content. It should be noted that for the sandy loam, the  $\gamma$  value remains almost constant as well.

During field experiments, utterly dry condition such as initial degree of saturation below 0.1 is rarely observed and infiltration tests are generally performed with initial soil condition higher but remaining relatively dry ( $Se_i < 0.3$ ). Therefore, some values of  $\beta$  and  $\gamma$  can be considered for the estimation of  $S$  and  $K_s$ . For the first group (sand and loamy sand textural soils),  $\gamma$  can be set to 0.9. Indeed, it is logical for very permeable soils to have a revised  $\gamma$  value higher than 0.75 because these soils have a behaviour quite close to a 1D flow. While for the second group, a default value of 0.75 can be kept. For the  $\beta$  parameter, the first group can have a value close to 0.9 which represents a mean value for this group. However, for the second group, it is not possible to fix a mean value for  $\beta$  value beforehand, as it varies from 0.72 to 2.32. Therefore, we propose to split this group in two:

sandy loam textural soils and the others (Loam, silty loam and silt) with respectively  $\beta$  values fixed to 0.75 and 1.5.

## 5 | CONCLUSIONS

In the debate on the constancy of the couplet ( $\beta, \gamma$ ), our study showed that these parameters are not constant and are influenced by the type of soil and the initial soil moisture. Our results indicate that synthetic soils can be classified into three groups: very draining soils with a reach of the permanent regime in less than 30 min (sand and loamy sand textural type), the second group where regime permanent is reached in less than 120 min (sandy loam textural type) and the others. For the first group and for relatively initially dry soil conditions (i.e.,  $Se_i < 0.3$ ), we suggest readjusting the by-default couplet from the case of ( $\beta = 0.6, \gamma = 0.75$ ) to ( $\beta = 0.9, \gamma = 0.9$ ). Note that the value of  $\beta = 1$  cannot be considered since it may lead to undefined numerical values with the use of the QEI model (see Equation 3) or the definition of the asymptote intercept (see Equation 4). For the second group (sandy loam textural soils), we propose to readjust the couplet to ( $\beta = 0.75, \gamma = 0.75$ ). For the last group who requests longer times for the attainment of the steady-state flow (over 120 min), the values ( $\beta = 1.5, \gamma = 0.75$ ) can be chosen as a good option for a more precise estimation of  $S$  and  $K_s$ . The results of this investigation are specific to the case of van Genuchten-Mualem soil hydraulic models and need to be tested on other models before generalization. The present work also highlights that there are two good options for the definition of the  $\gamma$  constant with 0.9 and 0.75. This means that a prefixed value for  $\gamma$  can be used when the transient expansion 3, 4 and 5 terms of the QEI and simultaneous estimate of triplet ( $K_s, S$  and  $\beta$ ) are considered. Although this work has focused on soil textural characteristics, new efforts should be made to study the possible influence of soil structure, for instance, compacted soils or high porosity soils such as technosols (Yilmaz, 2022) on  $\beta$  and  $\gamma$  values.

### DATA AVAILABILITY STATEMENT

The data that support the findings of this study are available from the corresponding author upon reasonable request.

### ORCID

D. Yilmaz  <https://orcid.org/0000-0003-0172-4767>

D. Moret-Fernandez  <https://orcid.org/0000-0002-6674-0453>

### REFERENCES

- Angulo-Jaramillo, R., Bagarello, V., Iovino, M., & Lassabatere, L. (2016). *Infiltration measurements for soil hydraulic characterization*. Springer.
- Bagarello, V., Di Prima, S., & Iovino, M. (2014). Comparing alternative algorithms to analyze the Beerkan infiltration experiment. *Soil Science Society of America Journal*, 78, 724–736. <https://doi.org/10.2136/sssaj2013.06.0231>
- Bagarello, V., Di Prima, S., & Iovino, M. (2017). Estimating saturated soil hydraulic conductivity by the near steady-state phase of a Beerkan infiltration test. *Geoderma*, 303, 70–77. <https://doi.org/10.1016/j.geoderma.2017.04.030>

- Brooks, R. H., & Corey, A. T. (1964). *Hydraulic properties of porous media*. Hydrology Paper No. 3. Civil Engineering Department, Colorado State University, Fort Collins, CO.
- Campbell, S. L., Chancelier, J. P., & Nikoukhah, R. (2010). Modeling and simulation in SCILAB. In *Modeling and simulation in Scilab/Scicos with ScicosLab 4.4* (pp. 73–106). Springer.
- Di Prima, S., Stewart, R. D., Abou Najm, M. R., Roder, R., Giadrossich, F., Campus, S., Angulo-Jaramillo, R., Yilmaz, D., Rogerro, P. P., Pirastru, M., & Lassabatere, L. (2021). BEST-WR: An adapted algorithm for the hydraulic characterization of hydrophilic and water-repellent soils. *Journal of Hydrology*, 603, 126936. <https://doi.org/10.1016/j.jhydrol.2021.126936>
- Di Prima, S., Stewart, R. D., Castellini, M., Bagarello, V., Abou Najm, M. R., Pirastru, M., Giadrossich, F., Iovino, M., Angulo-Jaramillo, R., & Lassabatere, L. (2020). Estimating the macroscopic capillary length from Beerkan infiltration experiments and its impact on saturated soil hydraulic conductivity predictions. *Journal of Hydrology*, 589, 125159. <https://doi.org/10.1016/j.jhydrol.2020.125159>
- Fuentes, C., Haverkamp, R., & Parlange, J. Y. (1992). Parameter constraints on closed-form soilwater relationships. *Journal of Hydrology*, 134(1–4), 117–142. [https://doi.org/10.1016/0022-1694\(92\)90032-Q](https://doi.org/10.1016/0022-1694(92)90032-Q)
- Haverkamp, R., Bouradui, F., Zammit, C., & Angulo-Jaramillo, R. (1999). Movement of moisture in the unsaturated zone. In *Groundwater engineering handbook*. CRC.
- Haverkamp, R., Debionne, S., Angulo-Jaramillo, R., & de Condappa, D. (2016). Soil properties and moisture movement in the unsaturated zone. In *The handbook of groundwater engineering* (pp. 167–208). CRC Press.
- Haverkamp, R., Parlange, J. Y., Starr, J. L., Schmitz, G., & Fuentes, C. (1990). Infiltration under ponded conditions: 3. A predictive equation based on physical parameters. *Soil Science*, 149(5), 292–300. <https://doi.org/10.1097/00010694-199005000-00006>
- Haverkamp, R., Ross, P. J., Smettem, K. R. J., & Parlange, J. Y. (1994). Three-dimensional analysis of infiltration from the disc infiltrometer: 2. Physically based infiltration equation. *Water Resources Research*, 30(11), 2931–2935. <https://doi.org/10.1029/94WR01788>
- Lassabatere, L., Angulo-Jaramillo, R., Soria-Ugalde, J. M., Šimůnek, J., & Haverkamp, R. (2009). Numerical evaluation of a set of analytical infiltration equations. *Water Resources Research*, 45(12). <https://doi.org/10.1029/2009WR007941>
- Lassabatere, L., Peyneau, P. E., Yilmaz, D., Pollacco, J., Fernández-Gálvez, J., Latorre, B., Moret-Fernández, D., Di Prima, S., Rahmati, M., Stewart, R. D., Abou Najm, M., Hammecker, C., & Angulo-Jaramillo, R. (2021). Scaling procedure for straightforward computation of sorptivity. *Hydrology and Earth System Sciences*, 25(9), 5083–5104. <https://doi.org/10.5194/hess-25-5083-2021>
- Lassabatere, L., Peyneau, P. E., Yilmaz, D., Pollacco, J., Fernández-Gálvez, J., Latorre, B., Moret-Fernández, D., Di Prima, S., Rahmati, M., Stewart, R. D., Abou Najm, M., Hammecker, C., & Angulo-Jaramillo, R. (2023). Mixed formulation for an easy and robust numerical computation of sorptivity. *Hydrology and Earth System Sciences*, 27(4), 895–915. <https://doi.org/10.5194/hess-2021-633>
- Latorre, B., Moret-Fernández, D., Lassabatere, L., Rahmati, M., López, M. V., Angulo-Jaramillo, R., Sorando, R., Comin, F., & Jiménez, J. J. (2018). Influence of the  $\beta$  parameter of the Haverkamp model on the transient soil water infiltration curve. *Journal of Hydrology*, 564, 222–229. <https://doi.org/10.1016/j.jhydrol.2018.07.006>
- Moret-Fernández, D., & Latorre, B. (2017). Estimate of the soil water retention curve from the sorptivity and  $\beta$  parameter calculated from an upward infiltration experiment. *Journal of Hydrology*, 544, 352–362. <https://doi.org/10.1016/j.jhydrol.2016.11.035>
- Moret-Fernández, D., Latorre, B., López, M. V., Pueyo, Y., Lassabatere, L., Angulo-Jaramillo, R., Rahmati, M., Torma, J., & Nicolau, J. M. (2020). Three- and four-term approximate expansions of the Haverkamp formulation to estimate soil hydraulic properties from disc infiltrometer measurements. *Hydrological Processes*, 34(26), 5543–5556. <https://doi.org/10.1002/hyp.13966>
- Mualem, Y. (1976). A new model for predicting the hydraulic conductivity of unsaturated porous media. *Water Resources Research*, 12(3), 513–522. <https://doi.org/10.1029/WR012i003p00513>
- Parlange, J. Y. (1975). On solving the flow equation in unsaturated soils by optimization: Horizontal infiltration. *Soil Science Society of America Journal*, 39(3), 415–418. <https://doi.org/10.2136/sssaj1975.03615995003900030019x>
- Parlange, J. Y., Lisle, I., Braddock, R. D., & Smith, R. E. (1982). The three-parameter infiltration equation. *Soil Science*, 133(6), 337–341. <https://doi.org/10.1097/00010694-198206000-00001>
- Rahmati, M., Vanderborght, J., Simunek, J., Vrugt, J. A., Moret-Fernández, D., Latorre, B., Lassabatere, L., & Vereecken, H. (2020). Soil hydraulic properties estimation from one-dimensional infiltration experiments using characteristic time concept. *Vadose Zone Journal*, 19(1), e20068. <https://doi.org/10.1002/vzj2.20068>
- Ross, P. J., Haverkamp, R., & Parlange, J. Y. (1996). Calculating parameters for infiltration equations from soil hydraulic functions. *Transport in Porous Media*, 24(3), 315–339. <https://doi.org/10.1007/BF00154096>
- Šimůnek, J., van Genuchten, M. T., & Šejna, M. (2008). Development and applications of the HYDRUS and STANMOD software packages and related codes. *Vadose Zone Journal*, 7(2), 587–600. <https://doi.org/10.2136/vzj2007.0077>
- Smettem, K. R. J., Parlange, J. Y., Ross, P. J., & Haverkamp, R. (1994). Three-dimensional analysis of infiltration from the disc infiltrometer: 1. A capillary-based theory. *Water Resources Research*, 30(11), 2925–2929. <https://doi.org/10.1029/94WR01787>
- Van Genuchten, M. T. (1980). A closed-form equation for predicting the hydraulic conductivity of unsaturated soils. *Soil Science Society of America Journal*, 44(5), 892–898. <https://doi.org/10.2136/sssaj1980.03615995004400050002x>
- Yilmaz, D. (2021). Alternative  $\alpha^*$  parameter estimation for simplified Beerkan infiltration method to assess soil saturated hydraulic conductivity. *Eurasian Soil Science*, 54, 1049–1058. <https://doi.org/10.1134/S1064229321070140>
- Yilmaz, D. (2022). Testing simplified Beerkan infiltration (SBI) methods on technosol to estimate the saturated hydraulic conductivity. *Geotechnical and Geological Engineering*, 40, 2897–2906. <https://doi.org/10.1007/s10706-022-02074-0>
- Yilmaz, D., Bouarafa, S., Peyneau, P. E., Angulo-Jaramillo, R., & Lassabatere, L. (2019). Assessment of hydraulic properties of technosols using Beerkan and multiple tension disc infiltration methods. *European Journal of Soil Science*, 70, 1049–1062. <https://doi.org/10.1111/ejss.12791>
- Yilmaz, D., Di Prima, S., Stewart, R. D., Abou Najm, M. R., Fernandez-Moret, D., Latorre, B., & Lassabatere, L. (2022). Three-term formulation to describe infiltration in water-repellent soils. *Geoderma*, 427, 116127. <https://doi.org/10.1016/j.geoderma.2022.116127>
- Yilmaz, D., Lassabatere, L., Angulo-Jaramillo, R., Deneee, D., & Legret, M. (2010). Hydrodynamic characterization of basic oxygen furnace slag through an adapted BEST method. *Vadose Zone Journal*, 9, 107. <https://doi.org/10.2136/vzj2009.0039>

**How to cite this article:** Yilmaz, D., Lassabatere, L., Moret-Fernandez, D., Rahmati, M., Angulo-Jaramillo, R., & Latorre, B. (2023). Soil-dependent  $\beta$  and  $\gamma$  shape parameters of the Haverkamp infiltration model for 3D infiltration flow. *Hydrological Processes*, 37(6), e14928. <https://doi.org/10.1002/hyp.14928>